



European Association of Urology



Trial Protocol

A Phase 3 Prospective Randomized Trial to Evaluate the Impact of Augmented Reality During Robot-assisted Radical Prostatectomy on the Rates of Postoperative Surgical Margins: A Clinical Trial Protocol

Gennaro Musi^{a,b,†}, Francesco A. Mistretta^{a,b,*,†}, Ottavio de Cobelli^{a,b}, Andrea Bellin^a, Gianluca Gaetano Vago^b, Gabriella Pravettoni^{b,c}, Danilo Bottero^a, Mattia Luca Piccinelli^a, Matteo Ferro^a, Mariia Ivanova^d, Giuseppe Petralia^{b,e}, Giulia Marvaso^{b,f}, Barbara A. Jereczek-Fossa^{b,f}, Vincenzo Bagnardi^g, Giuseppe Renne^d, Nicola Fusco^{b,d}, Stefano Luzzago^{a,b,*}

^a Department of Urology, European Institute of Oncology (IEO) IRCCS, Milan, Italy; ^b Department of Oncology and Hematology-Oncology, University of Milan, Milan, Italy; ^c Applied Research Division for Cognitive and Psychological Science, IEO, European Institute of Oncology IRCCS, Milan, Italy; ^d Division of Pathology, IEO European Institute of Oncology, IRCCS, Milan, Italy; ^e Precision Imaging and Research Unit, Department of Medical Imaging and Radiation Sciences, European Institute of Oncology (IEO), IRCCS, Milan, Italy; ^f Division of Radiotherapy, IEO European Institute of Oncology, IRCCS, Milan, Italy; ^g Department of Statistics and Quantitative Methods, University of Milan-Bicocca, Milan, Italy

1. Introduction and hypotheses

Accurate preservation of neurovascular bundles is crucial in guaranteeing erectile function recovery after robot-assisted radical prostatectomy (RARP) [1,2]. It is estimated that approximately 50% (32–68%), 65% (50–86%), and 70% (54–90%) of RARP-treated patients recover erectile function fully at 3, 6, and 12 mo after surgery, respectively [3]. However, the nerve-sparing approach during RARP is associated with higher rates of positive surgical margins (PSMs) at final pathology, especially in those tumors with extracapsular extension, and thus increasing the risk of biochemical recurrence (BCR) during follow-up [4,5]. Several preoperative tools are commonly used in daily practice for reducing PSM probability. For example, multiparametric magnetic resonance imaging (mpMRI) [6,7] and preoperative nomograms [8,9] have gained popularity for predicting tumor stage (cT2 vs cT3) and for intraoperative guidance during nerve-sparing dissection. Additionally, mpMRI information increases the accuracy of intraoperative frozen section (IFS) analysis of surgical margin status, which enables real-time histological monitoring of the oncological safety of a nerve-sparing procedure [10–12]. This said, today, none of

the mentioned tools have been shown to be completely reliable, and in consequence, novel technologies are required for implementing preservation of neurovascular bundles, while simultaneously decreasing the rates of PSMs. In this scenario of “precision prostate surgery,” three-dimensional (3D) virtual reconstruction of 2D cross-sectional imaging (mpMRI) has increasingly been adopted to facilitate the surgeon in better understanding the surgical anatomy [13]. Specifically, 3D reconstructions could be adapted and used in different settings: (1) virtual reality: the 3D model is visualized in a complete virtual environment; (2) mixed reality: through head-mounted display systems, the 3D model and the real environment can coexist and interact with each other; and (3) augmented reality (AR): the 3D model is overlapped over the real environment by a specific platform enhancing the real-world features [14].

In previous experiences, AR prostate surgery appeared to be safe and effective [15], and helped in correct surgical planning [16] and the identification of capsular involvement [17,18]. Moreover, two previous retrospective series [19,20] confirmed a 10–15% reduction in the rates of PSMs at final pathology, when AR RARP was compared with the standard approach. Finally, some authors hypothesized the

[†] These authors share co-first authorship.



use of AR to guide the IFS during RARP [20]. Despite these initial promising results, prospective studies are needed to demonstrate clinical utility and validate these technologies [21].

2. Design and protocol overview

This is a phase 3, monocentric, prospective, and randomized trial that compares AR RARP with the standard approach (standard RARP) for reducing the rates of PSMs at final pathology. The aim of this trial is to provide robust high-level data to establish whether AR RARP could guide a nerve-sparing approach and subsequent IFS analysis for reducing PSM rates, as compared with standard RARP. The working hypotheses of this trial are that the following: (1) AR RARP reduces the rates of PSMs at final pathology, if compared with standard RARP [19,20]; (2) a mixed reality IFS analysis of surgical margins provides a more precise tumor localization within the prostate gland [20]; (3) the reduced rates of PSMs with AR RARP will result in a significant management impact (ie, a clinically significant reduction in the percentage of PSMs); and (4) lower percentages in PSMs translates into greater oncological control (BCR) and greater recovery of erectile function after surgery.

The primary objective of this study is to compare the rates of PSMs with AR RARP versus standard RARP. The secondary objectives are the following:

1. To increase the rates of nerve-sparing approaches with AR RARP, if compared with standard RARP
2. To compare erectile function recovery at 3, 6, and 12 mo after surgery in AR RARP versus standard RARP
3. To compare the rates of PSMs in patients with organ-confined (pT2) and extraprostatic (pT3) disease in AR RARP versus standard RARP
4. To compare the size (mm) of PSMs in AR RARP versus standard RARP
5. To test the percentage of PSMs at the level of mpMRI lesions versus PSMs in other parts of the prostate in AR RARP versus standard RARP
6. To measure total surgical operative time in AR RARP versus standard RARP
7. To test the feasibility of the mixed reality IFS analysis of surgical margins in AR RARP
8. To test the percentage of IFS analysis positivity in mixed reality versus standard IFS
9. To evaluate the presence of tumor cells at the level of margin radicalization, in case of positive IFS, in AR RARP versus standard RARP.

A tertiary objective is to investigate the performance of confocal microscopy to evaluate intraoperative surgical margins and to compare its accuracy versus that of the standard IFS analysis (nonrandomized exploratory endpoint).

2.1. Patients and methods

We aim to evaluate the role of AR RARP, for reducing the rates of PSMs, in a patient population with good preoperative erectile function and interested in maintaining erections after surgery (Table 1). Preoperative

Table 1 – Study inclusion and exclusion criteria

Inclusion criteria	
Untreated, biopsy-proven adenocarcinoma of the prostate	
Age ≥ 18 yr	
EAU low- or intermediate-risk prostate cancer:	
1. PSA ≤ 20 ng/ml	
2. cT $\leq 2b$	
3. ISUP grade group $\leq III$	
Written informed consent provided for participation in the trial	
IIEF-5 ≥ 20	
No contraindications for mpMRI	
Exclusion criteria	
Any prior therapy for prostate cancer	
EAU high-risk prostate cancer:	
1. PSA > 20 ng/ml or	
2. cT $> 2b$ or	
3. ISUP grade group $> III$	
IIEF-5 < 20	
Prostate cancer with sarcomatoid or spindle cell or neuroendocrine small cell components	
Morbidity that would limit compliance with study protocols	
Contraindications to perform mpMRI	
EAU = European Association of Urology; IIEF-5 = International Index of Erectile Function-5; ISUP = International Society for Urological Pathology; mpMRI = multiparametric magnetic resonance imaging; PSA = prostate-specific antigen.	

clinical, biopsy, and imaging characteristics should indicate the safety of a nerve-sparing approach without compromising the oncological safety of the procedure. Patient population is defined as patients ≥ 18 yr old, with untreated biopsy-proven adenocarcinoma of the prostate classified as of European Association of Urology (EAU) low or intermediate risk (prostate-specific antigen [PSA] ≤ 20 ng/ml and cT $\leq 2b$ and International Society for Urological Pathology [ISUP] grade group [GG] $\leq III$) [22], with preoperative International Index of Erectile Function-5 (IIEF-5) ≥ 20 , and having no contraindications for mpMRI. A total of 318 patients will be recruited at a single center during approximately 3 yr. All patients should be followed for at least 1 yr after surgery.

The study is approved by the institutional review board of the European Institute of Oncology (number of registration IEO 1310) and sponsored by Università degli Studi di Milano (bando Mur per i Dipartimenti d'eccellenza 2018-2022, that was assigned to the Department of Oncology and Hematology-Oncology) and Medics Srl (Turin, Italy). This study will be conducted according to local regulations and laws, the ethical principles that have their origin in the Declaration of Helsinki, and the principles of Good Clinical Practice. Clinical data will prospectively be registered in an institutional database. The study is registered online (identifier: NCT06059859). The trial scheme is outlined in Figure 1.

2.2. Preoperative mpMRI

In both groups, all mpMRI examinations will be performed on a 3.0-T scanner (Avanto; Siemens Medical Solutions, Erlangen, Germany) with a phased-array coil. The mpMRI acquisition protocol will be compliant with the European Society of Urogenital Radiology (ESUR) guidelines [23]. Specifically, sagittal and axial T2-weighted images, axial diffusion-weighted images, and dynamic axial T1-weighted images after injection of contrast agent will be obtained. The analysis of mpMRI examinations will be performed by specialized radiologists with several years of experience in prostate mpMRI, following the Prostate Imaging Reporting and Data System (PI-RADS) v2.1 guidelines [24]. The probability of extraprostatic disease will be scored as suggested by the ESUR guidelines (ESUR-EPE score) [25].

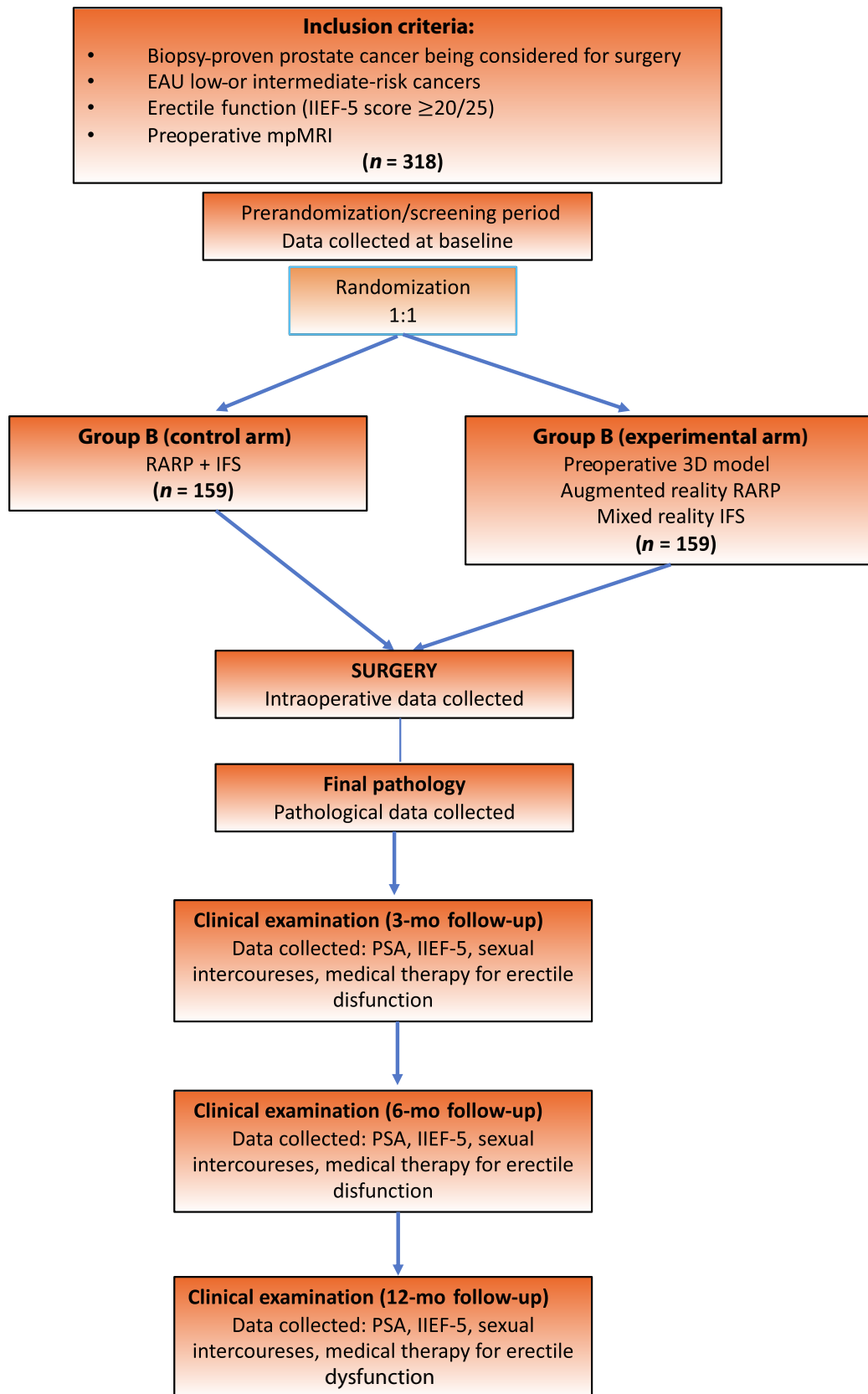


Fig. 1 – Trial schema. 3D = three dimensional; EAU = European Association of Urology; IFS = intraoperative frozen section; IIEF-5 = International Index of Erectile Function-5; mpMRI = multiparametric magnetic resonance imaging; PSA = prostate-specific antigen; RARP = robot-assisted radical prostatectomy.

2.3. Preoperative planning

After randomization, patients in the experimental arm will undergo 3D reconstruction of the prostate, according to preoperative mpMRI. Here, mpMRI images in Digital Imaging and Communications in Medicine (DICOM) format will be processed by Medics Srl (www.medics3d.com) to obtain a Hyper Accuracy 3D (HA3D) model, which is a patient-specific 3D reconstruction. Bioengineers will segment the mpMRI images using dedicated software (Mimics Medical 21.0; Materialise, Leuven, Belgium), and will create 3D reconstructions that accurately reproduce the prostate and the surrounding structures. More specifically, through the segmentation process, the prostate gland, urethra, urethral sphincter, neurovascular bundles, seminal vesicles, and prostate cancer lesions will be reconstructed. Once the HA3D model is obtained, a specific color will be assigned to each anatomical structure. All virtual models will be reviewed by bioengineers and urologists together to evaluate their accuracy in comparison with mpMRI (Fig. 2). In order to improve the spatial identification and localization of the lesion, the prostate gland will be subdivided in sectors. Each sector can roughly be approximated to a square with side length equal to 1 cm. The sector where the prostate cancer is localized will be colored differently from the prostate gland (Fig. 2). To identify the prostate anatomical areas, three stripes will also be represented: two horizontal orange stripes (Fig. 2) will subdivide the prostate in base, intermediate zone, and apex. The vertical cyan stripes (Fig. 2) will divide the prostate in anterior-posterior and left-right. Specific prostate structures can be hidden or turned transparent, in order to better visualize the tumor localization within the gland. Preoperatively, the HA3D model can be visualized, moved, and rotated using the Medics web portal (www.mymedics.com) or using a 3D pdf, which can be downloaded from the Medics web portal.

In the experimental arm, all surgeons will hypothesize a preoperative nerve-sparing approach, according to the mpMRI scan and before prostate 3D reconstruction visualization, respecting Tewari et al.'s [26] anatomical grades.

2.4. Surgery

All procedures will be performed by three highly experienced robotic surgeons (O.d.C.: 16 yr; G.M.: 13 yr.; and D.B.: 11 yr) respecting the technique described by Patel et al. [27] and using the Da Vinci surgical robot system (XI model; Intuitive Surgical, Sunnyvale, CA, USA) and a port device (Alexis; Applied Medical, Rancho Santa Margarita, CA, USA) system [28] for prostate extraction.

In the control group, all patients will undergo nerve-sparing dissection according to preoperative mpMRI images, as described previously [11,12]. Conversely, in the experimental group, a virtual image of the prostate will be overlapped onto the endoscopic view of the Da Vinci surgical robot system using the TilePro system (Fig. 3) [17]. Intraoperatively, to visualize and navigate the HA3D model, the intraoperative navigation software ICON (Intraoperative COgnitive Navigation system; Medics Srl) will be used [29,30]. Here, the overlap of the 3D models over the real anatomy during the nerve-sparing approach will be performed manually by a surgical assistant, with the support of a 3D professional mouse. The obtained merged images will be sent back to the Da Vinci remote console using the TilePro. All surgical procedures will aim to preserve the neurovascular bundles maximally, according to the patient's preoperative features. Total surgical time (in minutes) and final nerve-sparing anatomical grades according to Tewari et al. [26] will be annotated.

2.5. IFS analysis: inking margins

In the control group, after prostate extraction, surgeons will mark gland surface using a dermatographic pen in the areas where mpMRI indicated contact of the index lesion with the prostatic capsule [12].

Conversely, in the experimental arm, the explanted gland will be positioned on a plastic 3D support (Fig. 4) that allows for prostate rotation. Subsequently, Microsoft HoloLens head-mounted display system will be worn by the same surgeon. Specifically, mixed reality will be used to perfectly overlap the virtual 3D model of the prostate with the explanted gland. Again, a dermatographic pen will mark the areas where the 3D model indicated the contact of the index lesion with the prostatic capsule (Fig. 5).

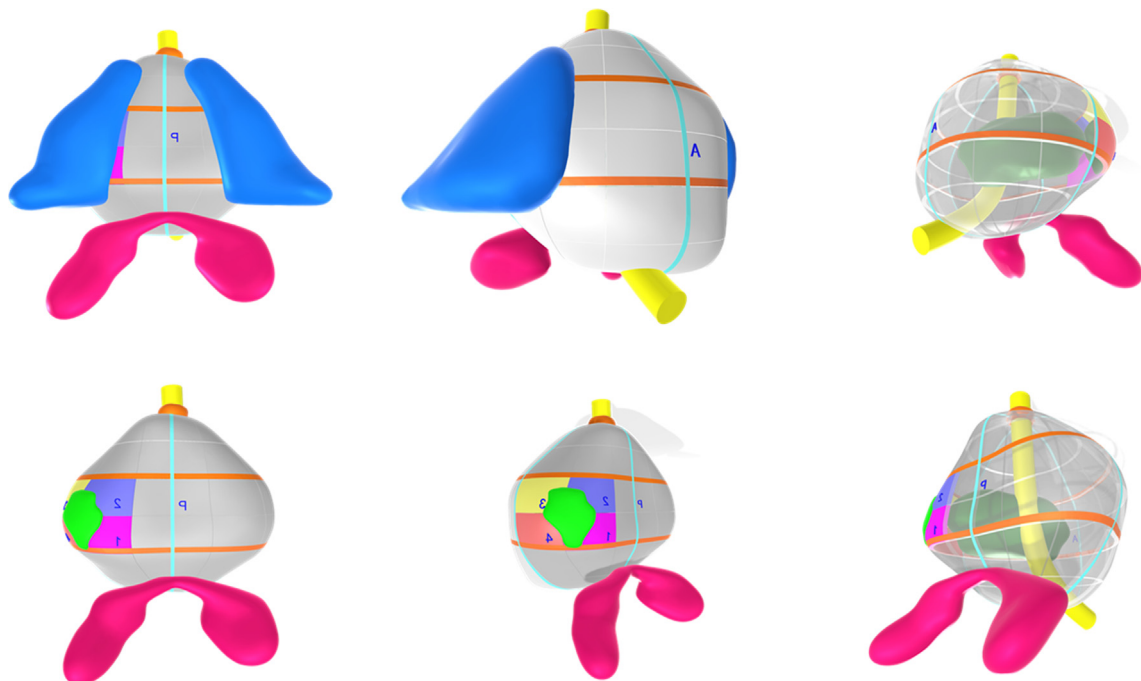


Fig. 2 – Examples of HA3D models. Color map: anterior prostate, light gray; posterior prostate, dark gray; urethra, yellow; urethral sphincter, orange; neurovascular bundles, blue; seminal vesicles, fuchsia; extracapsular prostate cancer, light green; intracapsular prostate cancer, dark green.

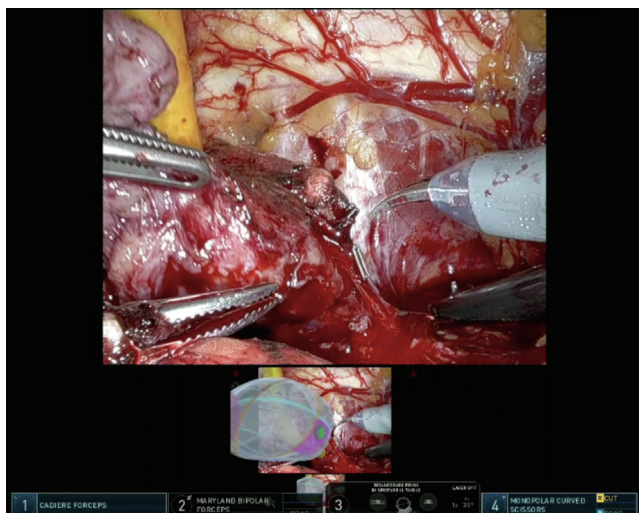


Fig. 3 – Example of augmented reality robot-assisted radical prostatectomy: nerve-sparing approach.

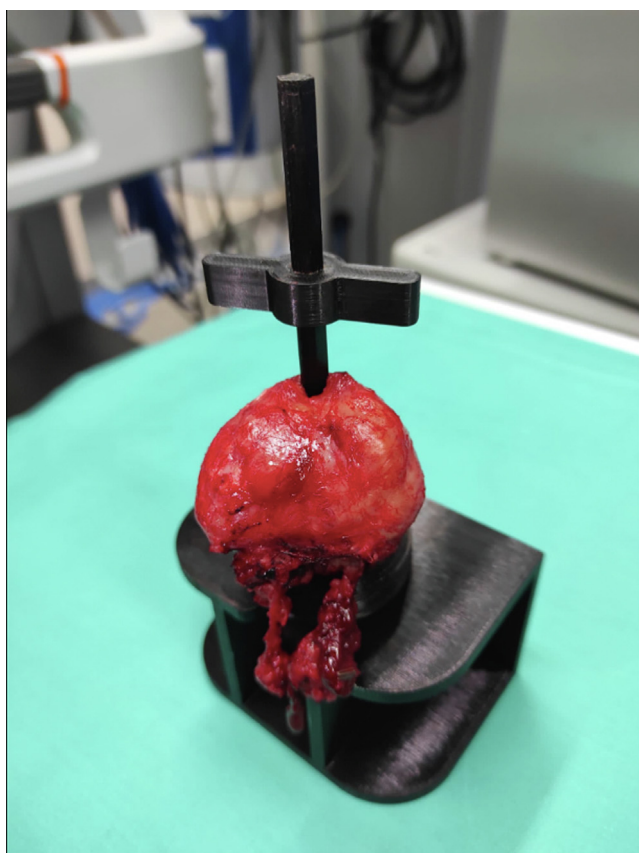


Fig. 4 – Explanted prostate is positioned on a plastic 3D support that allow for rotation. 3D = three dimensional.

2.6. IFS analysis: pathological evaluation

All prostatic samples will be analyzed by a dedicated uropathologist (G. R.) with several years of experience. In the control group, all marked areas will undergo IFS, as described previously [12]. The tissues for the IFS analysis (5- μ m sections) will be prepared for staining with hematoxylin and eosin for an optical microscopic examination. IFS results will

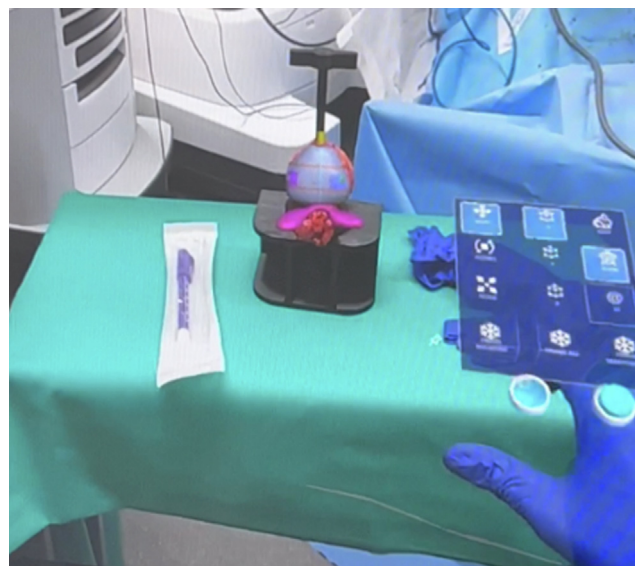


Fig. 5 – Inking prostate margins with mixed reality. Microsoft HoloLens head-mounted display system is used to overlap the virtual 3D model of the prostate to the explanted gland. 3D = three dimensional.

be reported as negative, positive (ink touching tumor cells; focally positive [≤ 1 mm]), “true” positive (>1 mm), or close surgical margin (cancer present within 0.1 mm of the inked margin).

The samples for the IFS analysis and the prostate specimen will then be fixed in formalin and analyzed for the final pathology report.

In the experimental group, before IFS, margins will be analyzed by confocal microscopy (exploratory analysis). Specifically, ex vivo fluorescence confocal microscopy (VivaScope 2500M-G4; Caliber I.D., Rochester, NY, USA) is an optical technology allowing examination of freshly excised tissue using fluorescence and reflectance techniques, providing a histological-like appearance of tissues. Specimens will be analyzed according to reports published previously [31,32]. Each prostate margin will be peeled (shaved) within the limits inked by surgeons. Slice will be immersed in 95% alcohol for 5–10 s, rinsed in 0.9% NaCl, soaked for 30 s in acridine orange 0.6 mmol/l and fast green (Sigma-Aldrich, Milan, Italy), and then embedded between two magnetic glass slides, with the surgical margin face in contact with the lower side. Sections will be flattened on the Vivascope for an en face analysis by using the lowest-thickness optical setup. Image results will be reported as negative (non-neoplastic extraprostatic muscle bundles, adipose tissue, nerves and prostatic inflammatory infiltrate, and prostatic glands with corpora amylacea and/or hyperplastic prostatic glands), positive (presence of prostate and periprostatic tissue with infiltrating growth within a nerve or atypical glands with prominent nucleolus and the absence of the basal cell layer), and doubtful (presence of prostate and periprostatic tissue with focal nucleolate atypical glands but without infiltrating growth; Fig. 6). Afterward, all specimens will undergo IFS (standard of reference).

2.7. Margin radicalization

In case of positive intraoperative margins, patients will undergo tissue radicalization. For men in the control group, surgeons will perform a secondary partial resection of the neurovascular bundle at the level of the positive area, as described previously [12]. Conversely, in the experimental arm, the virtual image of the prostate will again be overlapped in the prostatic fossa, and tissue radicalization will be superselective and tailored according to virtual models (Fig. 7). Secondary radicalizations will be sent for the final pathological examination.

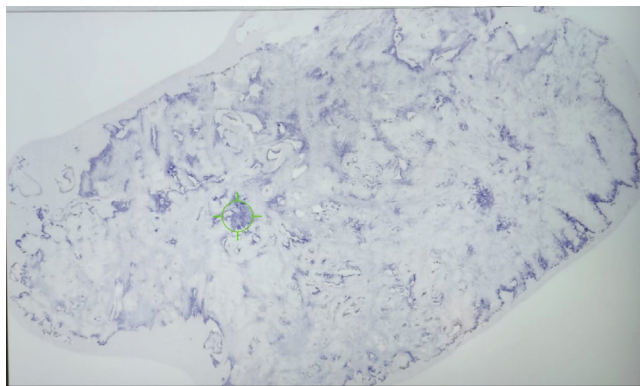


Fig. 6 – Example of a digital image obtained after analyzing prostate margins with the use of confocal microscopy (VivaScope 2500M-G4; Caliber I.D.).

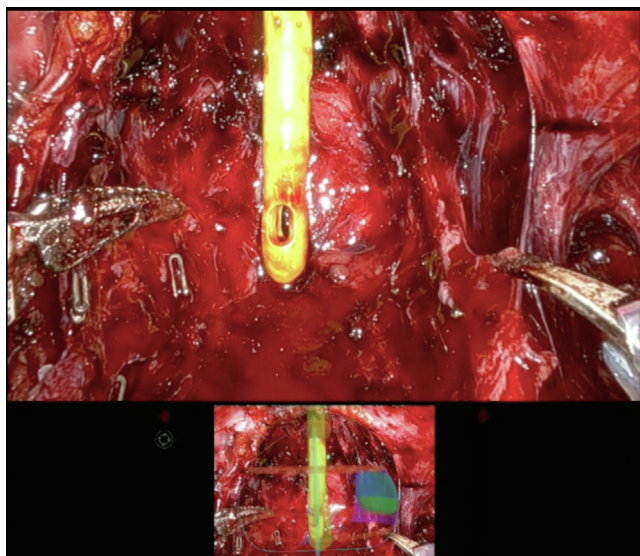


Fig. 7 – Example of augmented reality robot-assisted radical prostatectomy: margin radicalization.

2.8. Final pathology

All prostatectomy specimens will be processed with the whole mount methodology [33] and analyzed by the same dedicated uropathologist (G.R.). Tumors will be graded according to the ISUP GGs [34]. Pathological Tumor stage will be assigned by using the TNM classification system, eighth edition.

The surgical margins will be reassessed with the extension of any PSM determined according to the criteria of the Prostate Consensus Working Group [35]. Concordance between preoperative mpMRI and PSMs will also be evaluated.

2.9. Follow-up at 3, 6, and 12 mo

The following information will be recorded at 3-, 6-, and 12-mo follow-up: PSA, IIEF-5 questionnaire, sexual intercourse report (satisfaction, quality, percentage of complete sexual intercourses, etc.), documented use of any drug for erectile dysfunction, and patient general health status assessment. Early BCR will be defined at two consecutive PSA levels >0.2 ng/ml [36] within 1 yr from surgery.

3. Statistical analysis

Given the study design and a hypothetical expected difference of 10% between groups (20% PSMs in the control group vs 10% PSMs in the experimental group), to have adequate statistical power (80%), and considering an error of global first type with a tail of 5%, the required number is 159 patients per group [12,20]. The sample size calculation was performed assuming that the statistical test used for the comparison of proportions is a one-tailed Z test with pooled variance. Moreover, since the study's primary endpoint will be tested at the time of surgery, we did not consider a dropout rate in our sample size calculation to inflate the number of patients to be randomized in the study. In order to be able to stop the study for efficacy (stop for efficacy), an interim analysis on the main endpoint (percentage of PSMs) is foreseen. The interim analysis will be carried out when 50% of the total sample size is reached; to control the global type 1 error, the stop limit is set using the O'Brien-Fleming criterion. The interim analysis will be performed using an alpha error of 0.006 (in other words, the study can be stopped for efficacy if the one-sided p value comparing the proportion of patients with PSMs in the experimental versus control group will be <0.006), while in the final analysis, an alpha error of 0.048 will be used. Sample size calculations were performed using PASS 15 software.

Randomization of patients into the two arms will take place at the end of the patient's prehospitalization. Simple randomization, utilizing the randomizr package in R for generating the randomization list, will be applied. The outcome of the randomization will be communicated to the patient and the surgeon immediately before surgery.

4. Results

The study endpoints are summarized in Table 2.

4.1. Rates of PSMs

The presence of PSMs at final pathology in AR RARP versus standard RARP will be evaluated as the primary endpoint. The criteria of the Prostate Consensus Working Group [35] will be used for defining PSMs. A comparison between PSM percentages in AR RARP versus standard RARP will be performed with the chi-square test, and if required, multi-variable logistic regression models will be fitted. All tests will be performed as patient-level analyses. No strict indications for PSM management (adjuvant radiotherapy vs follow-up) will be provided for patients and clinicians.

Several subgroup analyses will subsequently be conducted to test whether AR RARP could provide a benefit in PSM reduction within all patient subcategories.

Comparisons in the percentage of PSMs between AR RARP and standard RARP will be performed in the following cases:

1. Organ-confined diseases (pT2) versus extracapsular diseased (pT3)

Table 2 – Study endpoints

<i>Primary endpoint</i>
Compare the rates of PSMs with AR RARP vs standard RARP
<i>Secondary endpoints</i>
Compare the rates of nerve-sparing approaches with AR RARP vs standard RARP
Compare erectile function recovery at 3, 6, and 12 mo after surgery in AR RARP vs standard RARP
Compare the rates of PSMs in patients with organ-confined (pT2) and extraprostatic (pT3) disease in AR RARP vs standard RARP
Compare the rates of PSMs, according to PI-RADS categories, in AR RARP vs standard RARP
Compare the rates of PSMs, according to ESUR-EPE categories, in AR RARP vs standard RARP
Compare the rates of PSMs, according to mpMRI lesion location, in AR RARP vs standard RARP
Compare the rates of PSMs in patients with clinically significant prostate cancer (ISUP GG ≥ 3) and nonclinically significant prostate cancer (ISUP GG 1–2) in AR RARP vs standard RARP
Compare the rates of PSMs in patients with EAU low- and intermediate-risk prostate cancer in AR RARP vs standard RARP
Compare the rates of PSMs, according to prostate volume, in AR RARP vs standard RARP
Compare the size (mm) of PSMs in AR RARP vs standard RARP
Compare the percentage of PSMs at the level of mpMRI lesions vs PSMs in other parts of the prostate in AR RARP vs standard RARP
Compare total surgical operative time (min) in AR RARP vs standard RARP
Feasibility of mixed reality IFS analysis of surgical margins in AR RARP
Compare the percentage of IFS analysis positivity in mixed reality vs standard IFS
Compare the presence of tumoral cells at the level of margin radicalization (secondary resections), in case of positive IFS, in AR RARP vs standard RARP
Proportion of changes in the nerve-sparing approach after 3D reconstruction visualization
<i>Tertiary endpoints</i>
Compare accuracy of confocal microscopy to evaluate intraoperative surgical margins vs the one of standard IFS analysis (nonrandomized exploratory endpoint)
AR = augmented reality; 3D = three dimensional; EAU = European Association of Urology; ESUR-EPE = European Society of Urogenital Radiology extraprostatic extension; IFS = intraoperative frozen section; ISUP GG = International Society for Urological Pathology grade group; mpMRI = multiparametric magnetic resonance imaging; PI-RADS = Prostate Imaging Reporting and Data System; PSM = positive surgical margin; RARP = robot-assisted radical prostatectomy.

- Clinically significant tumors (pathological ISUP GG ≥ 3) versus not clinically meaningful tumors (pathological ISUP GG 1–2) [37]
- PI-RADS categories (3 vs 4 vs 5)
- Multiparametric MRI index lesion location: base versus intermediate versus apex versus transitional zone
- Prostate volume: <80 versus ≥ 80 ml
- ESUR-EPE score categories: 1–2 versus 3 versus 4–5
- EAU risk categories: low versus intermediate

Finally, comparisons in PSM length (mm) and location (at the level of mpMRI index lesion vs in the other parts of the prostate) will be performed between AR RARP and standard RARP.

4.2. Management impact

For patients in the experimental arm, all surgeons will hypothesize a preoperative nerve-sparing approach, according to mpMRI images and before prostate 3D reconstruction visualization, respecting Tewari et al.'s [26] anatomical grades. After 3D model visualization (immediately before surgery) and at the end of surgical procedures, final nerve-sparing anatomical grades will be annotated. The proportion of patients requiring a change in the planned nerve-sparing approach (before and after 3D model visualization) will be tested.

4.3. Operative findings

Total surgical time (in minutes) in AR RARP versus standard RARP will be compared. Specifically, total surgical time will be evaluated as the time interval between skin incision and skin closure. No other specific time endpoints (ie, time for nerve-sparing dissection, etc.) will be calculated due to the variability in surgical approaches.

Final nerve-sparing approaches, according to Tewari et al.'s [26] anatomical grades, will be compared between AR RARP and standard RARP, using the chi-square test.

4.4. IFS analysis

The feasibility of mixed-reality IFS will be tested in the experimental arm. Surgeon will annotate the facility, their satisfaction, and comfort with the use of Microsoft HoloLens head-mounted display system for inking the prostate. Device malfunctions will also be annotated.

The rates of positive IFS will be compared between the experimental and control groups. Positive margin extension (focally positive ≤ 1 mm vs true positive >1 mm) between groups will also be compared.

4.5. Margin radicalization

The feasibility of AR margin radicalization in patients undergoing AR RARP will be evaluated. Again, surgeon satisfaction and the facility to use the device will be annotated. In order to compare the efficacy and the precision of AR margin radicalization versus standard radicalization, the percentage of patients with tumor cells present at the level of secondary resections will be compared between the two groups.

4.6. Tertiary endpoint

The accuracy of confocal microscopy to analyze intraoperative surgical margins will be evaluated as a tertiary endpoint (nonrandomized exploratory endpoint). In the experimental group, all patients will undergo a confocal microscopy analysis before standard IFS, as reported previously [31,32]. Pathologists will annotate the facility and their comfort in analyzing digital images. Image quality and the possibility to identify different prostate structures (ie, glands, tumor, nerves, etc.) within the digital image will also be considered. Finally, sensitivity, specificity, positive predictive value, negative predictive value, and accuracy of confocal microscopy versus standard IFS will be compared as a per-patient analysis.

4.7. Functional outcomes

Comparison of erectile function recovery at 3, 6, and 12 mo after surgery in AR RARP versus standard RARP will be performed. At every clinical examination, patients will again complete the IIEF-5 questionnaire (similar to that before surgery). The number of valid sexual intercourses and their quality, and patient satisfaction will be recorded and compared between groups. The use of oral drugs or other medical therapies for erectile dysfunction will be annotated.

4.8. Oncological outcomes

All patients will be followed for at least 12 mo after surgery. The percentages of early BCR (within 1 yr from surgery) between the two groups will be compared with Kaplan-Meier plots and log-rank tests.

5. Summary

Although two previous series have tested the use of AR RARP for reducing the rates of PSMs at final pathology [19,20], these analyses were limited by the retrospective nature and the enrolment of a limited number of cases. Furthermore, the use of mixed reality to guide the IFS analysis has been investigated poorly [20]. Despite these limitations, results from the literature suggest a 10–15% reduction in PSMs at final pathology, when AR RARP was compared with the standard approach [19,20]. It is therefore necessary to conduct a well-designed phase 3 prospective randomized trial to provide robust data on the utility of AR RARP in reducing PSM rates, while simultaneously guaranteeing correct preservation of neurovascular bundles.

In the short to medium term, the tailored nerve-sparing approach will improve erectile function recovery after surgery. In consequence, patient satisfaction, quality of life, and compliance to follow-up will also increase. Moreover, less use of medical drugs for erectile dysfunction could also result in a significant reduction of costs for the national healthcare system.

Since PSMs were previously associated with higher rates of disease recurrences over time [4,5], we advocate in better oncological control of prostate cancer with the use of AR RARP versus standard RARP. This outcome is particularly important, since it is frequently considered a surrogate of other major oncological endpoints (ie, BCR, clinical recurrence, and cancer-specific mortality). Moreover, lower rates of PSMs could also result in an important reduction of the use of adjuvant therapies after surgery or salvage therapies at the time of disease recurrence.

The trial has commenced, and we are actively recruiting patients. The first patient was randomized on January 6, 2022, and recruitment is processing on target. We believe that our study is innovative because it assesses the impact of AR RARP in reducing the rates of PSMs and the clinical utility of this innovative approach (ie, a significant reduction in PSMs). The trial will also enable us to establish whether AR RARP should replace the standard approach for all cases or whether it should be used in selected cases. The integration of the trial into the real-world practice will

provide a strong case for changing the conventional surgical approaches for prostate cancer.

Author contributions: Stefano Luzzago had full access to all the data in the study and takes responsibility for the integrity of the data and the accuracy of the data analysis.

Study concept and design: Musi, Mistretta, de Cobelli, Luzzago.

Acquisition of data: Piccinelli, Ferro.

Analysis and interpretation of data: Bellin, Renne, Ivanova, Bagnardi.

Drafting of the manuscript: Luzzago, Fusco.

Critical revision of the manuscript for important intellectual content: Vago, Pravettoni, Bottero, Marvaso.

Statistical analysis: Luzzago, Bellin.

Obtaining funding: None.

Administrative, technical, or material support: Bellin, Petralia, Jereczek-Fossa.

Supervision: Ferro.

Other: None.

Financial disclosures: Stefano Luzzago certifies that all conflicts of interest, including specific financial interests and relationships and affiliations relevant to the subject matter or materials discussed in the manuscript (eg, employment/affiliation, grants or funding, consultancies, honoraria, stock ownership or options, expert testimony, royalties, or patents filed, received, or pending), are the following: None.

Funding/Support and role of the sponsor: This work was partially supported by the Italian Ministry of Health with Ricerca Corrente and 5x1000 funds. Moreover, the trial was sponsored and funded by the Università degli Studi di Milano and by Medics Srl.

References

- [1] Walsh PC, Mostwin JL. Radical prostatectomy and cystoprostatectomy with preservation of potency. Results using a new nerve-sparing technique. *Br J Urol* 1984;56:694–7.
- [2] Walz J, Epstein JI, Ganzer R, et al. A critical analysis of the current knowledge of surgical anatomy of the prostate related to optimisation of cancer control and preservation of continence and erection in candidates for radical prostatectomy: an update. *Eur Urol* 2016;70:301–11.
- [3] Ficarra V, Novara G, Ahlering TE, et al. Systematic review and meta-analysis of studies reporting potency rates after robot-assisted radical prostatectomy. *Eur Urol* 2012;62:418–30.
- [4] Yossepowitch O, Briganti A, Eastham JA, et al. Positive surgical margins after radical prostatectomy: a systematic review and contemporary update. *Eur Urol* 2014;65:303–13.
- [5] Soeterik TFW, van Melick HHE, Dijkman LM, Stomps S, Witjes JA, van Basten JPA. Nerve sparing during robot-assisted radical prostatectomy increases the risk of ipsilateral positive surgical margins. *J Urol* 2020;204:91–5.
- [6] Park BH, Jeon HG, Jeong BC, et al. Influence of magnetic resonance imaging in the decision to preserve or resect neurovascular bundles at robotic assisted laparoscopic radical prostatectomy. *J Urol* 2014;192:82–8.
- [7] Alessi S, Pricolo P, Summers P, et al. Low PI-RADS assessment category excludes extraprostatic extension (\geq pT3a) of prostate cancer: a histology-validated study including 301 operated patients. *Eur Radiol* 2019;29:5478–87.
- [8] Nyarangi-Dix J, Wiesenfarth M, Bonekamp D, et al. Combined clinical parameters and multiparametric magnetic resonance imaging for the prediction of extraprostatic disease—a risk model for patient-tailored risk stratification when planning radical prostatectomy. *Eur Urol Focus* 2020;6:1205–12.

- [9] Patel VR, Sandri M, Grasso AAC, et al. A novel tool for predicting extracapsular extension during graded partial nerve sparing in radical prostatectomy. *BJU Int* 2018;121:373–82.
- [10] Schlomm T, Tennstedt P, Huxhold C, et al. Neurovascular structure-adjacent frozen-section examination (NeuroSAFE) increases nerve-sparing frequency and reduces positive surgical margins in open and robot-assisted laparoscopic radical prostatectomy: experience after 11,069 consecutive patients. *Eur Urol* 2012;62:333–40.
- [11] Bianchi R, Cozzi G, Petralia G, et al. Multiparametric magnetic resonance imaging and frozen-section analysis efficiently predict upgrading, upstaging, and extraprostatic extension in patients undergoing nerve-sparing robotic-assisted radical prostatectomy. *Med (United States)* 2016;95:e4519.
- [12] Petralia G, Musi G, Padhani AR, et al. Robot-assisted radical prostatectomy: multiparametric MR imaging-directed intraoperative frozen-section analysis to reduce the rate of positive surgical margins. *Radiology* 2015;274:434–44.
- [13] Porpiglia F, Amparore D, Checcucci E, et al. Current use of three-dimensional model technology in urology: a road map for personalised surgical planning. *Eur Urol Focus* 2018;4:652–6.
- [14] Amparore D, Piramide F, De Cillis S, et al. Robotic partial nephrectomy in 3D virtual reconstructions era: is the paradigm changed? *World J Urol* 2022;40:659–70.
- [15] Porpiglia F, Fiori C, Checcucci E, Amparore D, Bertolo R. Augmented reality robot-assisted radical prostatectomy: preliminary experience. *Urology* 2018;115:184.
- [16] Schiavina R, Bianchi L, Lodi S, et al. Real-time augmented reality three-dimensional guided robotic radical prostatectomy: preliminary experience and evaluation of the impact on surgical planning. *Eur Urol Focus* 2020;7:1260–7.
- [17] Porpiglia F, Checcucci E, Amparore D, et al. Three-dimensional elastic augmented-reality robot-assisted radical prostatectomy using hyperaccuracy three-dimensional reconstruction technology: a step further in the identification of capsular involvement. *Eur Urol* 2019;76:505–14.
- [18] Porpiglia F, Checcucci E, Amparore D, et al. Augmented-reality robot-assisted radical prostatectomy using hyper-accuracy three-dimensional reconstruction (HA3DTM) technology: a radiological and pathological study. *BJU Int* 2019;123:834–45.
- [19] Checcucci E, Pecoraro A, Amparore D, et al. The impact of 3D models on positive surgical margins after robot-assisted radical prostatectomy. *World J Urol* 2022;40:2221–9.
- [20] Bianchi L, Chessa F, Angiolini A, et al. Surgery in motion the use of augmented reality to guide the intraoperative frozen section during robot-assisted radical prostatectomy. *Eur Urol* 2021;80:480–8.
- [21] Wang S, Frisbie J, Keepers Z, et al. The use of three-dimensional visualization techniques for prostate procedures: a systematic review. *Eur Urol Focus* 2021;7:1274–86.
- [22] Mottet N, Bellmunt J, Briers E, et al. EAU-EANM-ESTRO-ESUR-ISUP-SIOG guidelines on prostate cancer. *Update* 2021;53:212.
- [23] Weinreb JC, Barentsz JO, Choyke PL, et al. PI-RADS Prostate Imaging – Reporting and Data System: 2015, version 2. *Eur Urol* 2016;69:16–40.
- [24] Turkbey B, Rosenkrantz AB, Haider MA, et al. Prostate Imaging Reporting and Data System version 2.1: 2019 update of Prostate Imaging Reporting and Data System version 2. *Eur Urol* 2019;2019:340–51.
- [25] Barentsz JO, Richenberg J, Clements R, et al. ESUR prostate MR guidelines 2012. *Eur Radiol* 2012;22:746–57.
- [26] Tewari AK, Srivastava A, Huang MW, et al. Anatomical grades of nerve sparing: a risk-stratified approach to neural-hammock sparing during robot-assisted radical prostatectomy (RARP). *BJU Int* 2011;108:984–92.
- [27] Patel VR, Shah KK, Thaly RK, Lavery H. Robotic-assisted laparoscopic radical prostatectomy: The Ohio State University technique. *J Robot Surg* 2007;1:51–9.
- [28] Almeida GL, Musi G, Mazzoleni F, et al. Intraoperative frozen pathology during robot-assisted laparoscopic radical prostatectomy: can ALEXIS™ trocar make it easy and fast? *J Endourol* 2013;27:1213–7.
- [29] Amparore D, Piramide F, Checcucci E, et al. Three-dimensional virtual models of the kidney with colored perfusion regions: a new algorithm-based tool for optimizing the clamping strategy during robot-assisted partial nephrectomy. *Eur Urol* 2023;84:418–25.
- [30] Ruzzenente A, Alaimo L, Conci S, et al. Hyper accuracy three-dimensional (HA3DTM) technology for planning complex liver resections: a preliminary single center experience. *Updates Surg* 2023;75:105–14.
- [31] Puliatti S, Bertoni L, Pirola GM, et al. Ex vivo fluorescence confocal microscopy: the first application for real-time pathological examination of prostatic tissue. *BJU Int* 2019;124:469–76.
- [32] Rocco B, Sarchi L, Assumma S, et al. Digital frozen sections with fluorescence confocal microscopy during robot-assisted radical prostatectomy: surgical technique. *Eur Urol* 2021;80:724–9.
- [33] Hollenbeck BK, Bassily N, Wei JT, et al. Whole mounted radical prostatectomy specimens do not increase detection of adverse pathological features. *J Urol* 2000;164:1583–6.
- [34] Epstein JI, Zelefsky MJ, Sjoberg DD, et al. A contemporary prostate cancer grading system: a validated alternative to the Gleason score. *Eur Urol* 2016;69:428–35.
- [35] Tan PH, Cheng L, Strigley JR, et al. International Society of Urological Pathology (ISUP) consensus conference on handling and staging of radical prostatectomy specimens. Working group 5: surgical margins. *Mod Pathol* 2011;24:48–57.
- [36] Cookson MS, Aus G, Burnett AL, et al. Variation in the definition of biochemical recurrence in patients treated for localized prostate cancer: the American Urological Association prostate guidelines recommendations for a standard in the reporting of surgical outcomes. *J Urol* 2007;177:540–5.
- [37] Gandaglia G, Ploussard G, Isbarn H, et al. What is the optimal definition of misclassification in patients with very low-risk prostate cancer eligible for active surveillance? Results from a multi-institutional series. *Urol Oncol* 2015;33:164.e1–e9.